Reduction of Wind and Swell Waves by Mangroves

Anna McIvor, Iris Möller, Tom Spencer
and Mark Spalding

Natural Coastal Protection Series: Report 1

Cambridge Coastal Research Unit Working Paper 40

The Nature Conservancy — Protecting nature. Preserving life.™   UNIVERSITY OF CAMBRIDGE   CCRU   WETLANDS INTERNATIONAL

Authors

Anna L. McIvor, The Nature Conservancy, Cambridge, UK and Cambridge Coastal Research Unit, Department of Geography, University of Cambridge, UK. Corresponding author: anna.mcivor@tnc.org

Iris Möller, Cambridge Coastal Research Unit, Department of Geography, University of Cambridge, UK.

Tom Spencer, Cambridge Coastal Research Unit, Department of Geography, University of Cambridge, UK.

Mark Spalding, The Nature Conservancy, Cambridge, UK and Department of Zoology, University of Cambridge, UK.

The Nature Conservancy's **Natural Coastal Protection** project is a collaborative work to review the growing body of evidence as to how, and under what conditions, natural ecosystems can and should be worked into strategies for coastal protection. This work falls within the Coastal Resilience Program, which includes a broad array of research and action bringing together science and policy to enable the development of resilient coasts, where nature forms part of the solution.

The **Mangrove Capital** project aims to bring the values of mangroves to the fore and to provide the knowledge and tools necessary for the improved management of mangrove forests. The project advances the improved management and restoration of mangrove forests as an effective strategy for ensuring resilience against natural hazards and as a basis for economic prosperity in coastal areas. The project is a partnership between Wetlands International, The Nature Conservancy, Deltares, Wageningen University and several Indonesian partner organisations.

About The Nature Conservancy

The mission of The Nature Conservancy is to conserve the lands and waters upon which all life depends. For general information, visit: www.nature.org. For more information about the Natural Coastal Protection project, visit: www.naturalcoastalprotection.org and www.coastalresilience.org.

About The Cambridge Coastal Research Unit

The Cambridge Coastal Research Unit is part of the Department of Geography in the University of Cambridge. It aims to provide the high quality scientific research to underpin sustainable coastal management. For more information, visit: http://www.ccru.geog.cam.ac.uk/ and http://www.geog.cam.ac.uk.

About Wetlands International

The mission of Wetlands International is to sustain and restore wetlands, their resources and biodiversity. Wetlands International is the only global non-profit organisation dedicated to the conservation and restoration of wetlands. It works through a network of 18 offices and many partners and experts to achieve its goals. For more information, visit http://www.wetlands.org/.

Executive Summary

Coastal populations are particularly vulnerable to the impacts of extreme events such as storms and hurricanes, and these pressures may be exacerbated through the influence of climate change and sea level rise. Coastal ecosystems such as mangrove forests are increasingly being promoted and used as a tool in coastal defence strategies. There remains, however, a pressing need to better understand the roles that ecosystems can play in defending coasts. This report focuses on mangrove forests and the role they can play in reducing wind and swell waves. While mangrove forests are usually found on shores with little incoming wave energy, they may receive larger waves during storms, hurricanes and periods of high winds. Large wind and swell waves can cause flooding and damage to coastal infrastructure. By reducing wave energy and height, mangroves can potentially reduce associated damage.

All evidence suggests that mangroves can reduce the height of wind and swell waves over relatively short distances: wave height can be reduced by between 13 and 66% over 100 m of mangroves. The highest rate of wave height reduction per unit distance occurs near the mangrove edge, as waves begin their passage through the mangroves.

A number of characteristics of mangroves affect the rate of reduction of wave height with distance, most notably the physical structure of the trees. Waves are most rapidly reduced when they pass through a greater density of obstacles. Mangroves with aerial roots will attenuate waves in shallow water more rapidly than those without. At greater water depths, waves may pass above aerial roots, but the lower branches can perform a similar function. The slope of the shore and the height of the waves also affect wave reduction rates through mangroves.
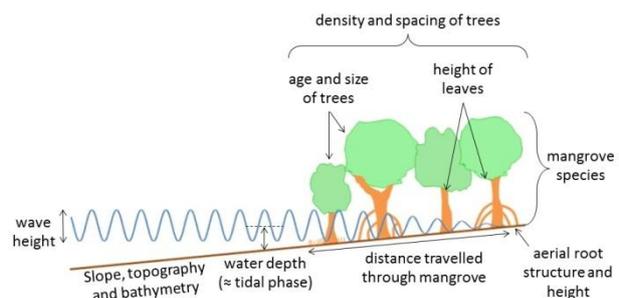
To understand the level of protection provided by mangroves, and to plan how to increase it, the passage of waves through mangroves has been modelled numerically using both a standard wave model used by coastal engineers called SWAN (Simulating WAves Nearshore) (Suzuki *et al*., 2011), as well as a model developed specifically for waves in mangroves called WAPROMAN (WAve PROpagation in MANgrove Forest) (Vo-Luong and Massel, 2008). These models are able to predict typical levels of wave attenuation given a knowledge of the mangrove characteristics, the wave parameters and the local bathymetry and topography. A statistical model has also been developed to explore the relationship between some standard forest measurements (tree height, tree density and canopy closure) and wave attenuation with distance (Bao, 2011). This model has been able to predict wave reduction within the Vietnamese mangroves where it was developed, and could be used to determine the width of mangrove belt needed to deliver a predefined level of protection from waves.

While there is a general confirmation that mangroves can attenuate wind and swell waves, research has focused on small waves (wave height < 70 cm), and there is a need to measure the attenuation of larger wind and swell waves associated with greater water depths, which may occur during storms and cyclones. More datasets are also needed to test the wider validity of the existing wave models under different wave conditions and in areas with different types of mangrove forest and different topographies.

CONTENTS

1. Introduction

The world's coastal margins are among the most densely populated and intensively used places on earth. Coastal populations are growing rapidly, as is associated infrastructure, industry and agriculture. These populations and coastal lands can be at risk from natural hazards such as waves, storms and tsunamis; the numbers of people at risk are increasing with the expansion of human populations, and the risks will likely be exacerbated by the effects of climate change and sea level rise.

Increasing attention is being given to adaptation in the coastal zone. An array of measures can help reduce the vulnerability of coastal populations, including: changes to planning and development patterns in near-shore zones; development of early warning systems and hazard response strategies; and coastal defence measures that maintain, enhance or develop structures or features that reduce the risk of impacts on coastal populations and lands.

Against this background there have been growing calls for the consideration of the role of natural coastal ecosystems in coastal defence. Claims have been made that some coastal ecosystems, including mangrove forests, coral reefs and salt marshes, can help to reduce the risk associated with some coastal hazards. Such ecosystems also provide a host of associated ecosystem services which may be lost if natural systems are replaced by built structures. If a case is to be made that ecosystems may be a realistic part of coastal adaptation, however, it will depend on having a solid science foundation, and on the ability to predict when, and under what conditions, the ecosystem may be able to function effectively as a defence against coastal hazards. This report comes as the first in a series of technical reports investigating the role of ecosystems in coastal defence.

Mangrove forests are increasingly being used or recommended as a part of broader coastal defence strategies. There remains, however, a growing need to better understand the roles that mangroves can play in defending coasts from hazards, such as wind and swell waves. Mangroves are found on many tropical coasts, mostly in locations with low incoming wave energy. However they can be exposed to much larger wind and swell waves during storms, hurricanes and periods of high winds. By reducing the energy of these incoming waves, mangroves reduce their impact on coastal infrastructure and the risk of flooding to those who live behind the mangroves. In doing so, they help to defend coasts from inundation and erosion, thus providing an important ecosystem service.

Maintaining this service is vital for coastal communities, but currently evidence for the ability of mangroves to reduce wind and swell waves is dispersed and often hard to find. This report aims to review available information about the capacity of mangroves to reduce wind and swell waves, in order to inform decision makers, planners and coastal engineers about the role mangroves can play in coastal defence against these hazards. Mangroves can also play a role in defending coasts from storm surges (Krauss *et al.*, 2009; Zhang *et al.*, 2012) and from erosion (Thampanya *et al.*, 2006); these roles are reviewed in the companion reports on these topics.

We begin by reviewing the capacity of mangroves to attenuate wind and swell waves. We look at evidence for wave attenuation in mangroves, and we review the factors affecting the rate of attenuation with distance. We then consider models that have been used to predict wave attenuation, and we look at what information is needed in order to use these models. Finally we look at how these models have been used to plan the use of mangroves in coastal defence strategies.

1.1 Waves

Wind and swell waves are the most common waves on the surface of the sea; Table 1 shows the different types of sea waves, along with the physical mechanisms producing these waves and their wave periods (the wave period is the time between two successive peaks passing a given point; see Figure 1 in Box 1). Wind and swell waves are formed by the action of the wind on the water surface in areas of open water; wind waves are generated near the coast, while swell waves are generated away from the coast, often travelling long distances before reaching the shore (Pugh, 1987; Woodroffe, 2002). Swell waves usually have longer wavelengths (e.g. 300 to 600m between successive peaks) and may have longer periods than locally generated wind waves (Pugh, 1987; Massel, 1996; Table 1). Boxes 1 and 2 provide more information on wave characteristics.

Table 1. Different types of waves, the physical mechanisms causing them and their wave periods (the time between two successive peaks passing a given point; see Fig. 1). From Massel (1996); Pugh (1987).

Wave type	Physical mechanism	Wave period
Wind waves	Wind shear, gravity	< 15 s
Swell waves	Wind waves	< 30 s
Tsunami	Earthquakes, landslides, submarine slumping	10 min – 2 hours
Tides	Gravitational action of the moon and sun, earth's rotation	12 – 24 hours
Storm surges	Wind stresses and atmospheric pressure variation in combination with local bathymetry and geomorphology (occur during storms, hurricanes, cyclones, typhoons)	1-3 days

1.2 Wave attenuation

Mangrove vegetation causes wave attenuation because it acts as an obstacle for the oscillatory water flow in the waves (Box 2), creating drag: as the water flows around the mangrove vegetation, it has to change direction and do work against the friction of the mangrove surface. This dissipates some of the energy of the waves, thereby reducing wave height (Box 1).

The rate of wave height reduction (r) per unit distance in the direction of wave propagation is defined as the reduction in wave height (ΔH) as a proportion of the initial wave height (H) over a distance (Δx) travelled by the wave (Mazda *et al.,* 2006):

$$r = -\frac{\Delta H}{H} \cdot \frac{1}{\Delta x} \qquad \textbf{Eqn. 1}$$

The units of r are /m or m^{-1}. For example, if wave height is reduced by 1% over a distance of 1 m, then $r = 0.01$ /m.

When r is constant, Equation 1 can be solved as:

$$H_x = H_0 . e^{(-r \cdot x)} \qquad \textbf{Eqn. 2}$$

where H_0 is the incident wave height (cm) and H_x is the wave height (cm) after the wave has travelled x metres (Mazda *et al.*, 2006).

A similar equation can be derived from wave theory (Han Winterwerp, pers. comm.):

$$H_x = H_0 . e^{k_i \cdot x} \qquad \textbf{Eqn. 3}$$

where k_i is the imaginary wave number. When this number is negative, the waves are being damped (i.e. they are reducing in height), while if this number is positive, waves are increasing in size.

Box 1. Wave characteristics

Waves can be characterized by their **height** (H) (which is twice their amplitude a), their **length** (L) (the distance from peak to peak or trough to trough), and their steepness, defined as H / L (as shown in Fig. 1; Park, 1999; Masselink *et al.*, 2011). The time between two successive peaks passing a given point is called the **period** (T) and the number of peaks (or troughs) passing a given point in a given time is known as the **frequency** (f). The sinusoidal waveform shown in Figure 1 is an idealized, monochromatic (single frequency) wave. In reality, waves vary in their height and length, and sea waves are usually made up of many component waves with different frequencies and amplitudes. A wave spectrum can be used to represent this mix (Park 1999; Masselink *et al.*, 2011).

To characterize real waves, the **significant wave height** $H_{1/3}$ or H_s is often used, which is calculated as the average height of the highest one-third of all waves occurring in a particular time period (Park 1999).

Waves propagate energy, rather than water, across space. While the water itself moves orbitally (Fig. 2), the waves propagate horizontally, carrying wave energy with them. The **energy** of a monochromatic wave is related to the square of its height:

$$E = \tfrac{1}{8} \rho \, g \, H^2 \qquad \textbf{Eqn. A}$$

where E is the energy per unit surface area (J/m^2), H is the wave height (m), ρ is the water density (kg/m^3) and g is the acceleration due to gravity (m/s^2) (Dean and Dalrymple 2002). The rate at which energy is supplied at a particular location (e.g. a beach) is called **wave power**, or energy flux, which is a product of wave energy E and wave group speed c_g (Park, 1999). **Wave attenuation** occurs when waves lose or dissipate energy, resulting in a reduction in wave height (Park 1999).
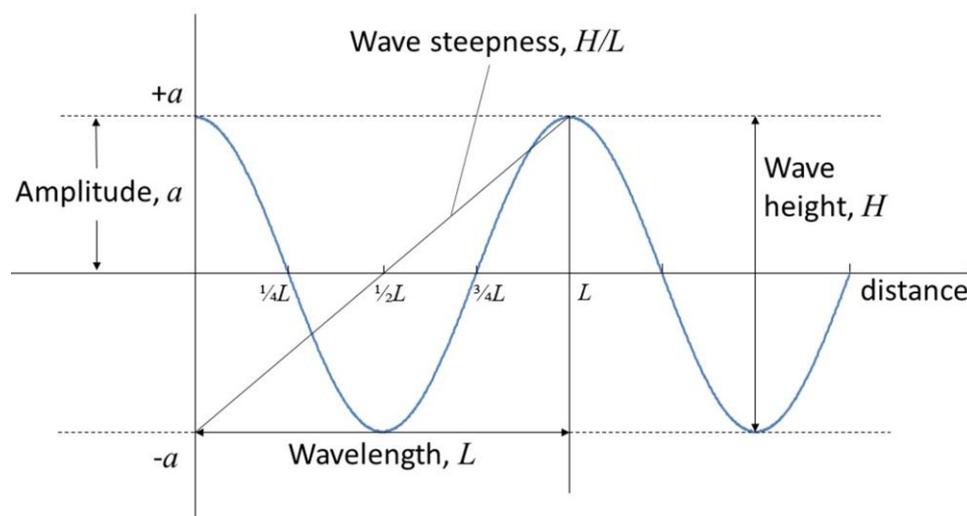
Figure 1. Vertical profile of an idealized (monochromatic) ocean wave, showing the linear dimensions and sinusoidal shape (adapted from Park, 1999).

Box 2. Waves approaching the shore

When wind waves approach the shore, the change in depth causes them to **shoal** i.e. they increase in height, maintaining their wave period but getting steeper. Advancing wave crests are slowed down more than successive crests until at some point, the waves **break** onto the shore, dissipating the energy in the wave. Waves become depth-limited when the depth of the water is approximately half the wavelength of the wave. At this point, the oscillatory motion of the water changes from circular oscillations to elliptical oscillations (Fig. 2).

As depth-limited waves approach the shore (before breaking), the only loss of energy occurs through bottom friction. In the absence of vegetation or an uneven substrate and in the presence of the shoaling process which increases wave height, bottom friction over a smooth bed (substrate) is not usually enough to cause a net reduction in wave height (i.e. wave attenuation). The presence of vegetation results in a drag force which greatly enhances wave attenuation compared to a smooth bed.
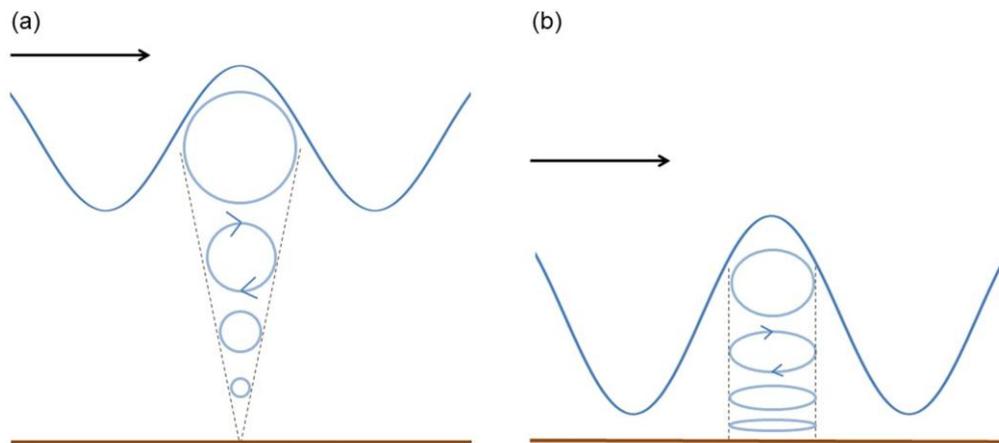
Figure 2. The movement of water within a wave. (a) Circular oscillatory motion when the wave is not depth-limited. (b) Elliptical oscillatory motion in a wave which is depth-limited. Adapted from Anderson *et al*. (2011).

2. Wave attenuation by mangroves

Studies that have measured the attenuation of wind and swell waves in mangroves are shown in Table 2. All these studies found a reduction in wave height as waves passed through mangroves. The level of wave attenuation varied between 0.0014 /m and 0.011 /m (Table 2). These attenuation rates suggest that across a 500 m width of mangrove forest, wave height would be reduced by 50 to 99%. These studies support the frequent assertion that mangroves can indeed attenuate wind and swell waves.

The studies are not directly comparable because other environmental parameters differed (e.g. incoming wave height, wave period, bottom slope (and thus shoaling effects), water depth). The studies measured the attenuation of relatively small waves (mostly less than 70 cm in height). Only Mazda *et al*. (2006) measured wave attenuation during a typhoon, when much larger waves can be present and when protection from waves is most important. Measurements of wave attenuation during storms and cyclones are rare; the harsh working conditions and extreme waves and surges that occur during storms make it difficult to carry out measurements in these environments. Also, experimental equipment left out during such storms can be lost (Granek and Ruttenberg, 2007).

Source	Location, measurements, species, wave period	How much did mangroves attenuate waves?	What did wave attenuation depend on?
Brinkman *et al.* 1997, Massel *et al.*, 1999	Time series of water surface elevation and flow along transects at Cocoa Creek, Australia and Iriomote Island, Japan. *Rhizophora stylosa* was the dominant mangrove species at Cocoa Creek, *Bruguiera* at Iriomote Island. Wave periods at Cocoa Creek varied between 1.5 and 4.5 s; most wave energy occurred in waves with periods of 1.5 to 3 s at Iriomote Island.	The wave energy transmission factor varies between 0.45 and 0.8 (where 1 is no loss of wave energy) 150 m into the forest. The transmission factor is the standard deviation of the wave energy spectrum at a point x divided by the standard deviation of the incident wave energy spectrum.	Peak wave energy transmission through mangroves depends on tidal level and structure of mangrove roots and trunks; when the projected area of obstructions from mangroves is high relative to total cross-sectional area of water flow, there is more drag. Wave energy transmission increases with water depth as there are fewer aerial roots higher up the tree.
Mazda *et al.* 1997a	Water levels and current velocities measured at several stations in the Tong King delta, Vietnam in areas planted with *Kandelia candel* or *Sonneratia caseolaris*. Swell waves with wave periods of 5 – 8 s.	Rate of wave height reduction up to 20% per 100m of mangroves (6 year old *Kandelia candel* trees that had been planted). Young mangroves (2 month old *Sonneratia caseolaris*) did not reduce waves.	High wave height reduction even when water depth increased because of high density of vegetation throughout the whole water depth.
Mazda *et al.* 2006	Water levels measured during the passage of a typhoon on the Vinh Quang coast in northern Vietnam; mangrove forests were made up of *Sonneratia* sp. Swell waves with periods of 8 – 10 s from a typhoon, maximum wave height approximately 40 cm.	Rate of wave height reduction varied between 0.0014 and 0.0058 per m cross-shore. The rate of wave reduction over 100 m of mangrove forest was calculated as 45% when water depth was 0.2 m and 26% when the water depth is 0.6 m.	Wave height reduction depended on tidal phase: at shallow water depths (low tides), wave reduction decreased with increasing depth because the pneumatophores taper off upwards; when water levels reached branch height, wave reduction increased, and was related to incident wave height.
Quartel *et al.* 2007	Current velocity and water level measured at three stations in the Red River Delta, Vietnam, with *Kandelia candel* the dominant mangrove species. Wave reduction compared over mangrove area and area with a sandy surface and embryonic cheniers. Wave periods 3.5 – 6.5 s.	Wave height reduction varied between 0.002 and 0.011 per metre cross-shore. The measured wave height reduction in the mangrove was higher than over the sandy surface.	Wave height reduction depended on water depth. The drag coefficient (C_D) among mangroves can be approximated by the function $C_D = 0.6\,e^{\,0.15A}$ (where A is the projected cross-sectional area of the under water obstacles up to a certain water depth).
Vo-Luong & Massel 2006, 2008	Pressure sensors and wave gauges placed along a transect at Nang Hai, Can Gio mangrove forest, southern Vietnam; forest consisted of mixed mangroves of *Avicennia* sp. and *Rhizophora* sp. in the first 100m; behyond this *Rhizophora* sp. dominated. There was a sharp drop in the level of the substrate at the edge of the mangroves (approx. 1.4m). A wave period of 1.2 s is assumed in the numerical model of wave reduction at this site. Incident wave heights were 0.35 – 0.4 m.	50-70% of the wave energy was dissipated in the first 20 m of mangrove forest when the water level (measured from the area without mangroves) was 1.9 and 2.1 m deep; 50% was dissipated over 40 m when water level was 2.5 m deep. After this initial drop, wave height continued to decrease only slightly.	The greatest reduction in wave height occurred as waves passed over the steep bank between mudflat and mangrove.
Bao, 2011	Wave attenuation measured in 32 plots in 2 coastal regions of Vietnam, the Red River Delta (northern Vietnam) and Can Gio mangrove forest (southern Vietnam). Wave height measured at 6 points along a 120m transect from forest edge. 6 mangrove species present. Initial wave heights between 20 to 70 cm (wave periods not given).	Mean wave height reduction (calculated using data from graphs in Bao, 2011) was 0.0054/m over 80m of mangrove forest.	71% of the variation in the slope coefficient (related to the rate of wave attenuation with distance into forest) was associated with the mangrove forest structure (height and density of mangroves and canopy closure). Southern mangroves provide more protection per m of forest.

Table 2. Wave attenuation studies in mangroves. Because wave attenuation has been measured in different ways at different sites, it is not possible to present wave attenuation in a standardised way across the different sites.

3. Factors affecting wave attenuation in mangroves

The factors known to affect the reduction in wave height as waves pass through mangroves include water depth, which is a function of topography/bathymetry and tidal phase, wave height, and various aspects of the structure of mangrove trees, which depend on their species, age and size (Fig. 3, Table 2). These factors are discussed in more detail below.
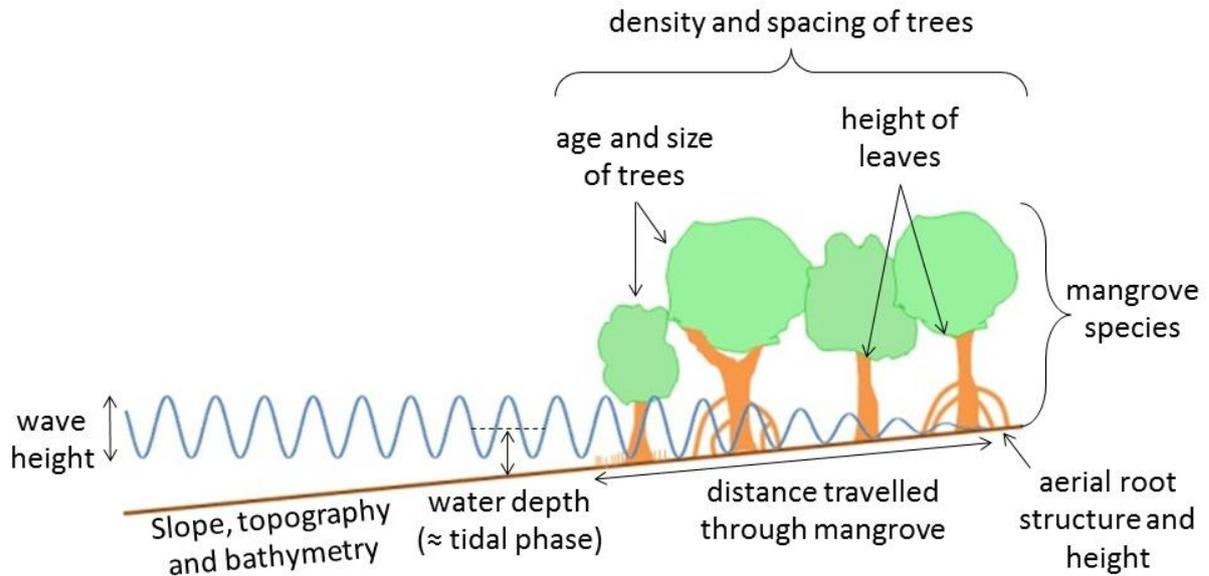
Figure 3. Factors affecting wave attenuation in mangroves.

3.1 Distance travelled through mangrove

Waves passing through mangrove forests show an exponential reduction in height with distance (Fig. 4; Bao, 2011). Bao (2011) studied wave height reduction in several plots in Vietnam (Table 2). Wave heights were measured along 92 transects distributed among 32 plots divided into 2 areas, and the exponential regression equations were highly significant, with $R^2 > 0.95$ and $p < 0.001$ (Fig. 4). The mean wave height reduction over the first 40 m of forest was 21% and over the next 40 m was 17%, with a total reduction of 35% over the first 80 m of forest (raw data not given, so these means are calculated from data given in Figures 4 and 5 of Bao, 2011).

3.2 Water depth relative to structure of mangrove trees

The most important factors affecting the rate of wave attenuation with distance in mangroves are water depth (which is related to tidal phase) and the structure and characteristics of the mangrove vegetation. Together, these determine the nature of obstacles encountered by waves as they pass through the mangrove forest. In the following section we go through some different mangrove morphologies, looking at how wave attenuation with distance varies with water depth.
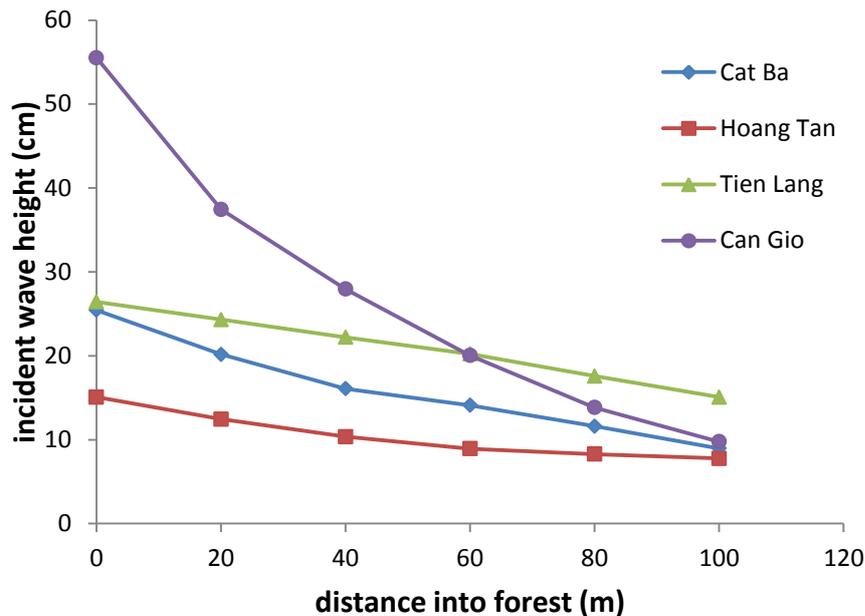
Figure 4. The variation in wave height with distance travelled through mangrove forests in 4 sample locations in Vietnam, from Bao (2011). Regression equations for these 4 locations were as follows: Cat Ba: $H_x = 24.9\ e^{-0.01x}$, $R^2 = 0.99$; Hoang Tan: $H_x = 14.3\ e^{-0.007x}$, $R^2 = 0.97$; Tien Lang: $H_x = 27.2\ e^{-0.006x}$, $R^2 = 0.98$; and Can Gio: $H_x = 54.8\ e^{-0.02x}$, $R^2 = 0.99$ (Bao, 2011).

3.2.1 Prop roots
***Rhizophora* spp.** have prop roots, which form a network above the substrate (Fig. 5, left image). These prop roots present considerable resistance to the flow of water. Above the prop roots, the trunks present less of an obstacle to waves, allowing them to pass more easily. This results in high wave attenuation at shallow depths, and then a reduction in wave attenuation as the water becomes deeper and the waves are less affected by the prop roots.

This pattern was seen by Brinkman *et al.* (1997) at Cocoa Creek in Australia (Fig. 6a, Table 2), where *Rhizophora stylosa* is the dominant species over the 180m of mangrove forest nearest to the shore. When the tide was rising and the waves were passing through the prop roots, less than half the peak wave energy was transmitted through the first 80m of mangrove (water depths 1.25m at the forest edge and 0.5m at a point 80m into the forest). Brinkman *et al.* note that at these shallow depths, the projected area of obstructions to the flow caused by above-ground roots was only slightly smaller than the total cross-sectional area of the flow, so they would have created significant drag (the projected area is the area of the silhouette of mangrove vegetation as seen from the direction of the on-coming waves). As the water level increased, wave energy was transmitted further into the forest: at high tide, almost 50% of the peak wave energy was transmitted through to a point 80m into the forest. At these water depths, the ratio of the projected area of obstructions to the total cross-sectional area of flow decreases because the water is now higher than the prop roots, so that the waves experience less drag and there is less wave attenuation.

3.2.2 Knee roots
While the knee roots of ***Bruguiera* spp.** are quite dissimilar in structure to the prop roots of *Rhizophora* spp., they nevertheless attenuate waves in a similar way. Brinkman *et al.* (1997) found that wave height reduction was greatest at shallow depths; in deeper water, wave heights were reduced less with distance, and more wave energy was transmitted further into the forest on Iriomote Island, Japan (Fig. 6a).

11

Figure 5. Left: Prop roots of *Rhizophora stylosa* near Cairns, Queensland, Australia. Right: Pneumatophores of *Sonneratia alba*, Bangkok, Thailand. (*Rhizophora* photo by Justin Meager, used with permission. *Sonneratia* photo by Tony Rodd, used under the Creative Commons license.)

3.2.3 Pneumatophores

Sonneratia **spp.** and *Avicennia* **spp.** have characteristic pneumatophores, aerial roots which project out of the substrate and support an air supply to the roots. The aerial roots of *Avicennia* are narrow and can reach 20 to 30cm in height. *Sonneratia* aerial roots have secondary thickening and so are more cone-shaped, reaching over a metre in height in some species (Fig. 5, right image).

Like the prop roots of *Rhizophora* spp. and the knee roots of *Bruguiera* spp., the pneumatophores of *Sonneratia* act as obstacles to water movement at shallow depths, creating higher wave attenuation at these depths. Mazda *et al*. (2006) measured wave attenuation in a mangrove forest created by planting *Sonneratia* in northern Vietnam. They found the highest attenuation at shallow depths, and lower wave attenuation as water levels rose (Fig. 6b), until the water levels reached the height of the branches and leaves (see next section).

3.2.4 Trunks, branches and leaves

Many mangrove species do not have aerial roots, such as *Kandelia candel* and *Nypa fruticans*. As waves pass through these species, wave attenuation is expected to be lower in shallow water depths, as the waves will only encounter the trunks or base of the trees. At higher water depths, when the waves reach the branches and leaves, wave attenuation is expected to increase.

Quartel *et al*. (2006) measured wave attenuation in coastal mangroves in the Red River Delta, Vietnam (Table 2), where *Kandelia candel* is the dominant species. They found that the rate of wave reduction increased with water depth (Fig. 6c). They also measured mangrove trunk height and width and foliage height and width, and used these to estimate the projected area of mangroves to incident waves at different water depths. They plotted the projected area (silhouette) against the drag coefficient C_D; the drag coefficient is a measure of the resistance to flow, and can be calculated from the water level, wave heights and distance travelled by waves using equations given in Mazda *et al*. (1997a) and in section 4.3 below. They showed that the resistance to flow increased with the projected area of obstacles (Fig. 7), and that the drag coefficient could be approximated by the function $C_D = 0.6 \, e^{0.15A}$ (where A is the projected cross-sectional area of the underwater obstacles up to a certain water depth).

Mazda *et al*. (2006) found a similar pattern in *Sonneratia* spp. in Vietnam. At higher tidal levels, when the water levels allowed the waves to pass through the branches and leaves of the trees, wave attenuation increased, although there was a very high degree of scatter in the data (Fig. 6b).

Mazda *et al.* (2006) suggest that this increase in wave attenuation at higher water depths was due to the thickly spread branches and leaves dissipating the wave energy. When the water level reached the height of the branches and leaves, wave attenuation was also influenced by wave height (see section 3.4 below).
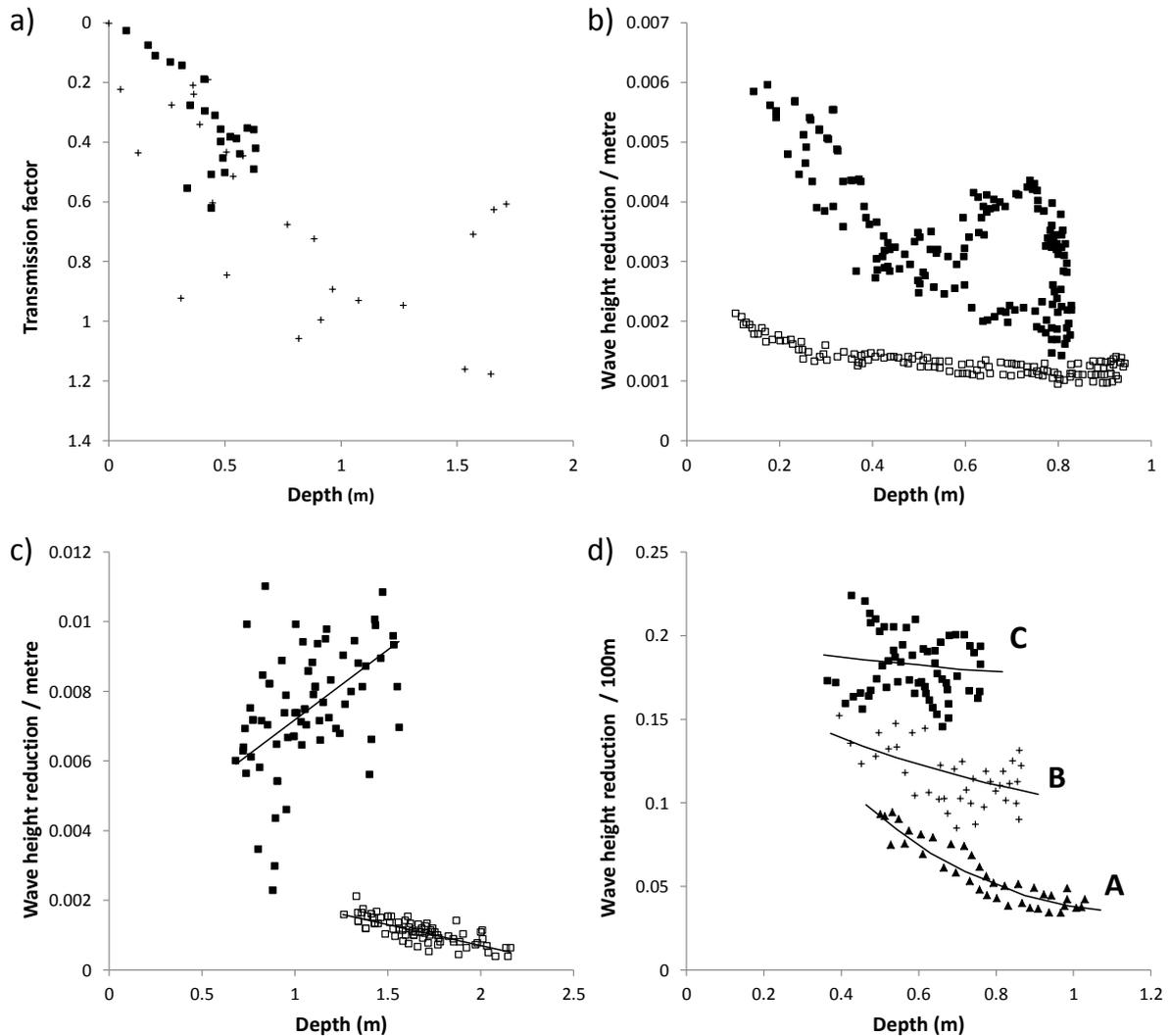
Figure 6. (a) The transmission of wave energy plotted against water depth in a mangrove forest dominated by *Bruguiera* sp. on Iriomote Island (■) and by *Rhizophora stylosa* at Cocoa Creek (+) from Brinkman *et al.* (1997); a low transmission factor shows high wave attenuation (note that the y-axis has been reversed so that the pattern can be compared with the other graphs). (b) Wave height reduction plotted against depth in a mangrove forest dominated by *Sonneratia* sp. (mangrove forest (■) and area without mangroves (□), data from Mazda *et al.* 2006). (c) Wave height reduction in a forest dominated by *Kandelia candel* (mangrove forest (■) and area without mangroves (□), data from Quartel *et al.* 2007). (d) Wave height reduction in an area recently planted with *Kandelia candel*, showing reduction through 6-month-old saplings (▲, area A), 3-4 year-old trees (+, area B) and 5-6 year-old trees (■, area C) (data from Mazda *et al.*, 1997a). See also Table 2, which gives more details about these studies.

13
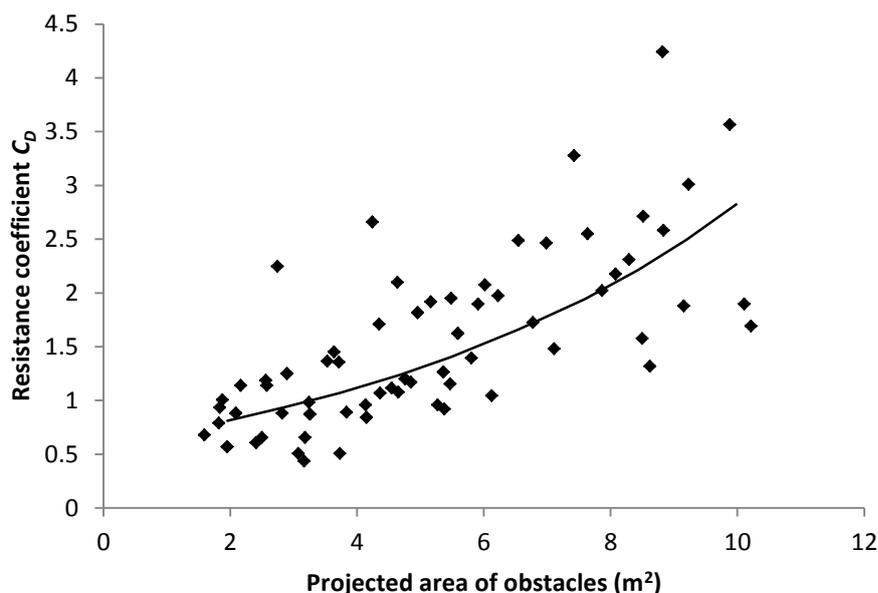
Figure 7. Variation of the drag coefficient (also called the resistance coefficient) with the projected area of obstacles (i.e. mangrove vegetation) to the incoming waves for *Kandelia candel* in the Red River Delta, Vietnam, taken from Quartel *et al.* (2007).

3.2.5 The age of trees

The age of the trees is important in determining their ability to attenuate waves, mediated by their size, shape and the density of trunks, branches and aerial roots. Mazda *et al.* (1997a) measured wave attenuation in a recently planted *Kandelia candel* area (Fig. 6d). The trees in this area were in three bands of different aged trees parallel to the shore, with the youngest band containing 6 month-old seedlings (area A), the next band containing 3-4 year-old trees (area B), and the final band containing 5-6 year-old trees (area C). Wave attenuation through the youngest trees decreased with increasing depth, as would be expected if no mangrove trees had been present: when no obstacles are present, wave attenuation depends on bottom friction alone, so at greater depths, bottom friction becomes less important and less wave attenuation occurs (shown in Fig. 6b and 6c in the control areas). Amongst the older trees, wave attenuation was higher, and it decreased less with increasing depth, implying that bottom friction was becoming less important and friction caused by the mangrove vegetation was having a greater effect. As the trees get larger still, the leaves and branches will play a larger role until wave attenuation increases with depth (as seen in Fig. 6c with older *Kandelia candel* trees).

3.2.6 Summary

A central factor affecting wave attenuation in mangroves is the density of obstacles that waves encounter as they pass through the mangrove, and the height of these obstacles relative to the water depth. As the depth of the water increases, the projected area of the obstacles will also increase, providing the obstacles are taller than the water depth. The wave attenuation will depend on the projected area of obstacles as a proportion of the total underwater cross-sectional area, and also the position of the obstacles relative to the water surface: if the obstacles are mostly near the ground and the water is deep, then the majority of the water motion will be unaffected by the obstacles and little wave attenuation will occur. Calculations of the projected area of mangroves at different heights above the ground should therefore allow the estimation of the wave attenuation properties of mixed species assemblages.

3.3 Shore slope and topography

The slope of the shore is a central factor affecting energy dissipation in waves, influencing water depth and hence wave shoaling and breaking. Mangroves often grow on very gently sloping shores, and no studies have been found that have specifically looked at the effect of slope on wave energy dissipation in mangroves. By encouraging sedimentation over the longer term, mangroves can increase surface elevation, thereby creating shallower water, increasing wave shoaling and energy dissipation (this is covered in the companion report on surface elevation change in mangroves).

In some areas, the combination of erosion and the effect of mangrove roots binding the soil together has resulted in the formation of a scarp (a sharp change in surface elevation) at the edge of the mangroves. This results in a sudden change in water depth, which affects wave height. Vo-Luong and Massel (2006) measured wave attenuation in an area with a 1.2 m high ledge at the margin between the mangroves and the lower shore in the Can Gio mangrove forest, south Vietnam. This step change in height resulted in a sudden reduction in water depth when the tide was high enough to reach the mangrove area, and a sharp decrease in significant wave height was observed within 20m of the mangrove edge. When the water level is lower, the margin acts like a small sea wall, and wave energy dissipates against the exposed mangrove roots or is reflected back out to sea (this is likely to cause erosion of the mangrove area).

It should be noted that such topographic features can lead to a shoaling effect, i.e. an increase in wave height due to a decrease in water depth, without the breaking of waves, and thus a temporary increase in wave energy over the scarp; this has been observed across cliffed margins between mudflats and more landward saltmarsh surfaces higher up in the tidal frame (Möller and Spencer 2002).

3.4 Wave height and period

The effect of wave height and wave period on wave attenuation in mangroves has not been studied, except in the case where water levels reach mangrove branches and leaves, as described below. Brinkman *et al*. (1997) found that there were no significant changes in the energy spectrum of waves of different periods as the waves passed through mangroves; this implies that waves of different periods were attenuated at a similar rate. In the absence of evidence to the contrary, we assume in this report that shorter period wind waves and longer period swell waves are attenuated at similar rates as they pass through mangroves.

Mazda *et al.* (2006) showed that the rate of wave height reduction was dependent on the initial wave height when the water level reached the mangrove branches and leaves. Large waves were attenuated more (Fig. 8). Their measurements were made during a 3 hour period of constant water depth, with small waves (significant wave height between 11 and 16cm) passing through *Sonneratia* spp. in northern Vietnam. By contrast, in the area without mangroves, wave reduction was independent of wave height (Fig. 8).

Mazda *et al.* (2006) hypothesize that the wave motion has been transformed into turbulence and eddies through the interaction with the branches and leaves, dissipating the wave energy. Extrapolating from the data in Figure 8, they predict that when water depths reach the height of the branches and leaves, and with a significant wave height of 20cm, the rate of wave reduction with distance would be 0.006 /m, equivalent to a 50% reduction in wave height as waves pass 100m through the mangroves. However they note that this effect is only significant when the waves are passing through the branches and leaves, and that the wave period will also affect the rate of energy dissipation (wave period was approximately 9 s in this study).

15

Unlike the mangrove trunks, aerial roots and larger branches, smaller branches and leaves are flexible and this will affect their interaction with waves. The relationship between wave height and wave attenuation may be different at different water levels (e.g. if the waves do not reach the leaves) and in mangroves of different species and ages (this will affect whether waves are passing through roots, trunks or branches and leaves).
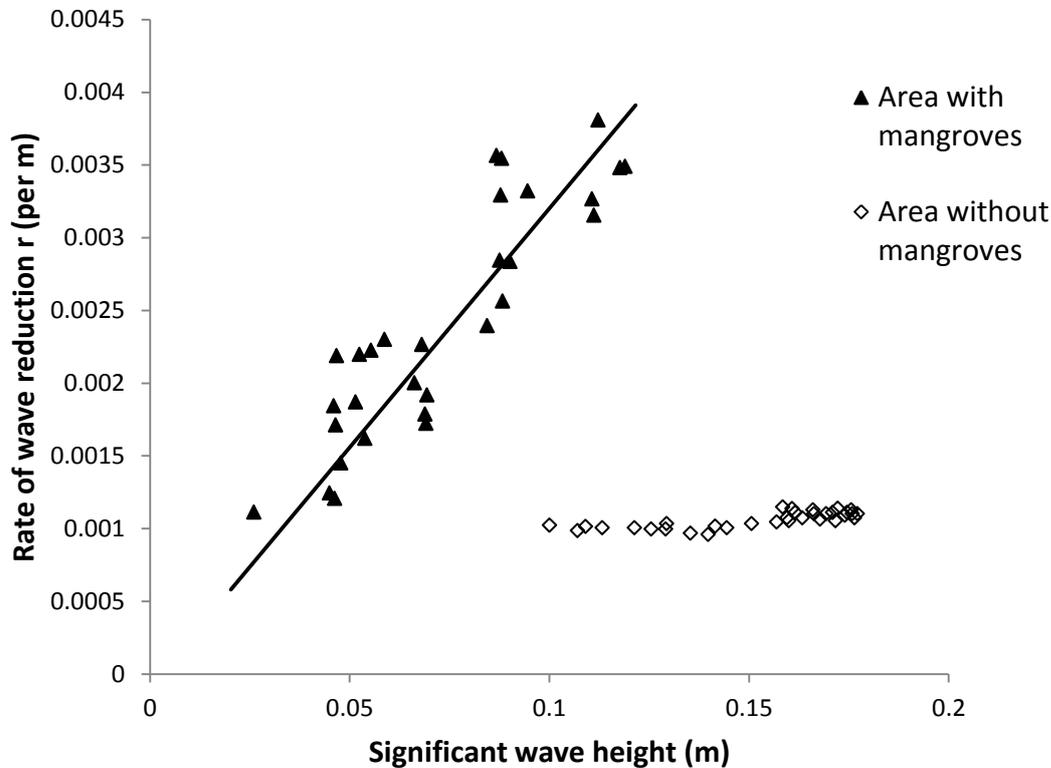
Figure 8. How wave attenuation varies with wave height, from Mazda *et al.* 2006, plotted using measurements taken over a 3 hour period when the water depth remained constant.

3.5 Other factors affecting wave energy dissipation

There are a variety of other factors that are likely to affect the rate of wave attenuation within mangroves, such as the state of the tide, tidal flows, and the arrangement of the trees (i.e. clumped or dispersed). Mangroves are also likely to reduce wave set-up (the increase in water level that occurs as waves push water onto the shore), and the effect of the wind on the water, thus preventing waves reforming or increasing in size within mangrove areas (Costanza *et al.*, 2008).

4. Modelling the dissipation of wave energy through mangroves

Numerical and statistical models of wave attenuation in mangroves have been developed to facilitate better understanding and prediction of the behaviour of waves in mangroves.

Three modelling approaches have been developed to predict the reduction of waves passing through mangroves:
1. the WAPROMAN model developed by Vo-Luong and Massel (2008);
2. an adaptation of the SWAN model (Booij *et al.* 1999), developed by Suzuki *et al.* (2011);
3. a regression model based on observations of wave attenuation in Vietnamese mangroves, developed by Bao (2011).

These models are described below. Both the WAPROMAN and adapted SWAN models are based on quantifying the work done by the movement of water on plant stems. This approach has been widely used to quantify wave reduction by vegetation (reviewed in Anderson *et al*. 2011).

4.1 The WAPROMAN model

Massel *et al*. (1999) developed a predictive model of wave propagation through mangrove forests. Mangrove trunks and roots were treated as cylindrical elements located in the water column (leaves are not included). Interactions between vegetation elements were included in the drag force by modifying the drag coefficient depending on the density of trunks and roots. This initial model assumed that the forest was uniform (i.e. similar tree morphology throughout the mangrove forest) and had constant water depth (i.e. no change in surface elevation). The resulting rate of wave attenuation depended strongly on the density of the mangrove forest, the diameter of mangrove roots and trunks and the characteristics of the incident waves. Hadi *et al*. (2003) used this model to compare wave attenuation in *Rhizophora* and *Ceriops* forests, and concluded that the *Rhizophora* forest was more effective at attenuating waves.

Vo-Luong and Massel (2008) further refined the model, and named it the WAPROMAN model: WAve PROpagation in MANgrove forest. The revised model allows for a sloping or uneven surface and mangrove species can vary at different locations and can have different densities. Wave-trunk interactions and wave breaking are the dominant factors reducing waves.

The WAPROMAN model requires the following input parameters:
- topography measured along a transect parallel to the direction of on-coming waves (they use 1 m – 2 m intervals);
- wave height, wave period and spectrum of incident waves; and
- characteristics of mangrove trees measured in different horizontal layers (e.g. aerial root layer, trunk layer, canopy layer) and different areas of the forest; to include the number and diameters of trunks or aerial roots in every layer in every area.

Vo-Luong and Massel (2008) tested the model using experimental wave data from a study in Nang Hai mangrove forest, Can Gio biosphere reserve, southern Vietnam (Vo-Luong and Massel, 2006). Observed wave dissipation was roughly in agreement with the model results, after an adjustment for density of mangroves had been made, which probably reflected the actual densities along their transects (Fig. 9).

4.2 Modelling wave dissipation in vegetation using SWAN

Dalrymple *et al*. (1984) modelled wave dissipation through vegetation, treating the vegetation elements as vertical cylinders in water of constant depth, and using a bulk drag coefficient to account for approximations and factors not considered in their formula (Suzuki *et al*. 2011). Mendez and Losada (2004) expanded this to narrow-banded random waves, and included wave damping and wave breaking over vegetation fields at variable depths, taking into account the geometric and physical characteristics of the vegetation. Suzuki *et al*. (2011) implemented the Mendez and Losada (2004) equation in the SWAN model (Simulating WAves Nearshore), a third-generation wave model that computes random, short-crested wind-generated waves in coastal regions (Booij *et al*., 1996 & 1999; SWAN, 2011; TU Delft, 2011); it is freely available on the internet (http://swanmodel.sourceforge.net/) and is used by coastal engineers to model wave dynamics. Suzuki *et al*. (2011) extended the model to include vertical layers such as those seen in mangroves (e.g. bottom layer containing aerial roots, higher layers containing leaves and branches), and horizontal variation in vegetation characteristics (e.g. due to different species being present in different areas).
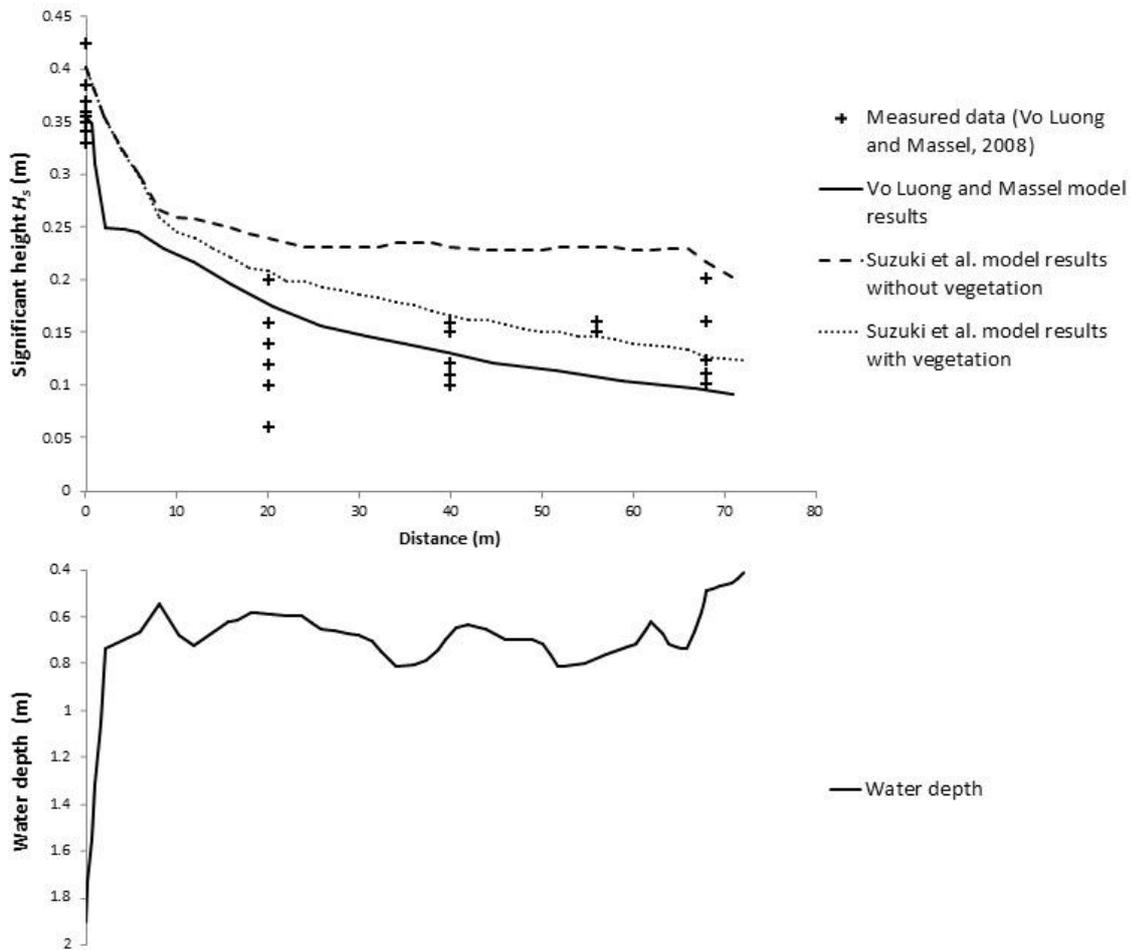
Figure 9. Measurements of significant wave heights at Nang Hai mangrove forest, Can Gio Mangrove Biosphere Reserve in southern Vietnam (water depth 1.9m; Vo-Luong and Massel, 2008), plotted alongside the outputs from 2 models, the WAPROMAN model of Vo-Luong and Massel (2008) and the SWAN model adapted by Suzuki *et al.* (2011). The SWAN model was run with and without vegetation to explore the effects of the mangroves on the waves (Suzuki et al., 2011). The water depth is shown in the bottom panel (Vo-Luong and Massel, 2008). See both Vo-Luong and Massel (2008) and Suzuki *et al.* (2011) for similar graphs at different water depths. Figure adapted from Vo-Luong and Massel (2008) and Suzuki *et al.* (2011).

To apply the model to a mangrove area, it is necessary to know the stem diameter of vegetation elements (i.e. aerial roots, trunks, branches), the number of vegetation elements per square metre and the bulk drag coefficient, which depends on the wave characteristics, the hydrodynamic regime and the vegetation characteristics. If insufficient data are available on these, Suzuki *et al.* (2011) suggest using a vegetation factor, V_f, defined as the product of stem diameter, density and the bulk drag coefficient, which could be measured for each location (although it would change with time as plants grew). Where good vegetation data are available, the bulk drag coefficient is the only other factor in the wave model that needs to be calibrated over a range of wave characteristics and hydrodynamic conditions, and must be calibrated separately for each vegetation layer. Model inputs also include wave height, wave period and a parameter that describes wave breaking.

Suzuki *et al*. (2011) demonstrate the application of their model using the data of Vo-Luong and Massel (2008) (used in the WAPROMAN model above). The model also shows a reasonable fit with the observed data (Fig. 9).

Suzuki *et al*. (2011) note that the model is capable of calculating wave diffraction around vegetation patches. While their model does not include vegetation motion and the effects of plant flexibility, it could represent the effect of mangrove canopies if their bulk drag coefficient was measured (Tomohiro Suzuki, pers. comm.). Other models of wave dissipation through vegetation address the issue of vegetation motion and flexibility: for example, Asano *et al*. (1993) model wave dissipation through submerged beds of swaying vegetation; these models have yet to be combined with models of wave dissipation through mangroves.

4.3 The drag coefficient

The model of Vo-Luong and Massel (2008) does not require parameterization with a drag coefficient, as this is approximated based on the Reynolds number (a dimensionless number which is widely used to describe the flow of fluids around objects) of trunks and roots, as described in Massel *et al*. (1999); however Massel *et al*. note that their approximation is only valid where vegetation density is between 9 and 49 stems or roots per m^2. The model of Mendez and Losada (2004) depends on a single parameter similar to the drag coefficient used by Dalrymple *et al*. (1984); the parameter is a function of the local Keulegan-Carpenter number for a specific type of plant (the Keulegan-Carpenter number is a dimensionless number describing the relative importance of the drag forces over inertia forces for bluff objects in an oscillatory fluid flow). The model of Suzuki *et al*. (2011) requires a bulk drag coefficient, but offers the alternative of using a calibrated vegetation factor which also takes stem diameter and density into account.

Clearly the measurement, calculation or approximation of the drag coefficient is an essential element of these models. Several attempts have been made to calculate the drag coefficient of coastal vegetation using other parameters which are easier to measure, such as vegetation characteristics; these are reviewed in Anderson *et al*. (2011).

A relationship between the bulk drag coefficient and the Reynolds number has been found by Kobayashi *et al*. (1993) using data from the artificial kelp experiments of Asano *et al*. (1988), and by Mazda *et al*. (1997b) using data recorded during tidal flows in mangroves swamps in Nakama-Gawa, Iriomote Island, Japan and Coral Creek, Hinchinbrook Island, Australia. In both cases, the drag coefficients decrease exponentially as the Reynolds number increases.

In freshwater systems, the bulk drag coefficients of common wetland species have been measured and reference values are available for use in flow calculations through floodplains (e.g. Fischenich and Dudley, 2000). A bulk drag coefficient has been measured for mangrove forests of some species (Mazda *et al*. 1997a & 1997b; Quartel *et al*. 2007). These studies used the following equation, derived by Mazda *et al*. (1997a), to calculate the drag coefficient (or resistance coefficient, C_D) using incident wave height measured in front of mangroves (H_0), wave height at an in-shore location having passed through mangroves (H_x), and the distance (x) and the mean depth (h) between the two stations:

$$C_D = \frac{32\sqrt{2}}{\pi} \frac{h^2}{H_1 \Delta x}\left(\frac{H_0}{H_x} - 1\right) \qquad \textbf{Eqn 4}$$

This equation is an approximation for longer waves such as swell waves in shallow water, and is derived from equations describing the flow resistance caused by bottom friction (Mazda *et al*. 1997a). The values for the drag coeffficient vary with depth of water, as the waves pass through different parts of the vegetation (i.e. aerial roots or trunks). The drag coefficients for these different layers of the mangrove forest have not been measured separately, as would be needed for these drag coefficients to be used in the SWAN model adapted by Suzuki *et al*. (2011). This is an area that needs further research.

4.4 A regression model to predict wave attenuation in mangroves

General mangrove characteristics have also been used to predict wave attenuation in mangrove forests. Bao (2011) used various characteristics of the forest structure to predict wave height at different distances from the forest edge using the following regression model, based on measured wave heights (described in Table 2):

$$H_x = (0.9899\, H_0 + 0.3526)\, .\, e^{(0.048 - (0.0016\, TH)\, - (0.00178\, \ln\, (TD)) - (0.0077\, \ln\, (CC))\, .\, x} \qquad \textbf{Eqn 5}$$

where H_x is wave height a distance x into the forest (measured in cm), H_0 is incident wave height (measured in cm), *TH* is average tree height (m), *TD* is tree density (no. of trees / hectare), and *CC* is canopy closure (%) (see Bao (2011) for more details about this method). The advantage of using average tree height, tree density and canopy closure to predict wave attenuation is that these are easy and quick to measure. Bao's model is intended for use with mangroves in Vietnam; the relationship between these forest parameters and wave attenuation will need to be studied in other areas in order for this approach to be used more widely. The model was created using data from small waves (wave heights less than 70 cm) so care also needs to be taken before extrapolating the model to predict attenuation of larger storm waves by mangroves.

4.5 Application of models

The following case studies show how these models can be used as tools to plan the use of mangroves to protect coastal communities and structures from wind and swell waves. In the first case study, the SWAN model was used to predict wave attenuation at a port behind a mangrove island, and different configurations of the mangrove island were tested to see if changes to the shape and size of the island would increase wave attenuation (Narayan, 2009; Narayan *et al*. 2010). In the second case study, a mangrove forest structure index was used to predict the width of mangroves required in different areas of Vietnam in order to reduce a 3 m high wave to a height of 0.3 m (Bao, 2011).

4.5.1 Case study 1: Predicting wave attenuation behind a mangrove island

Narayan *et al*. (2010) use the modified SWAN model of Burger (2005) and Suzuki *et al*. (2011) to estimate wave attenuation at Dhamra port behind Kanika Sands mangrove island, Orissa, India, for cyclone-induced wind waves of varying return periods (Figure 10; see Narayan (2009) for a more detailed description of the study). They used the modified SWAN 40.81 model described in section 4.2 (Suzuki *et al*. 2011), and the following parameter estimates:

- Nearshore wave heights and periods were estimated using data from 13 cyclone events. Storm surge levels were estimated for different return periods by extrapolating available data. Significant wave heights varied between 4 and 7 m, storm surge heights between 4 and 9 m, and peak wave periods (i.e. the period of the waves containing the most energy) between 12 and 17 s at a depth contour of -11 m; the range of values represent the different return periods, with the smallest values being for a return period of 5 years, and the highest values for a return period of 100 years (Narayan *et al*., 2010).

- Offshore bathymetry, estimated using hydrographic maps, was used to calculate the transfomation of waves moving from deep to shallow water.
- Mangrove vegetation was generalized as being *Rhizophora mucronata*; the vegetation factor needed by the model was calculated using previous measurements of root, stem and canopy diameters, densities and heights from the literature and local experts, and assuming a drag coefficient of 1, based on the Reynolds number of water flow within a mangrove vegetation patch being of the order of 1 x 10^5 under cyclone conditions (Narayan, 2009).

Wave height transformations were calculated for waves with different return periods (5, 25 and 100 years) and different angles of approach (22.5°, 45° and 90° to the coast).

For a wave height with a return period of 25 years and an incident wave angle of 90°, a wave reduction of nearly 50% was observed at the port due to the effect of the mangrove island; attenuation within the island was nearly 90%, but a relatively sharp recovery of wave heights was seen beyond the island, partially because of the island's shape (Fig. 11). Because of the presence of the mangrove vegetation on the island, 2.5 m waves have a calculated return period of 60 years at Dhamra Port, compared to a return period of 20 years if the mangrove island was not present.

Narayan *et al.* (2010) also used the model to explore the effects of the mangrove island being made wider, and of mangroves being present in a strip around the margin of the island (but not in the middle of the island). They concluded that an extension of the vegetation on the northern side of the island would decrease wave height at the port. A 300m wide band of dense mangrove vegetation around the outside of the island showed only a small difference in wave attenuation as compared to the protection provided by the fully vegetated island.

Narayan *et al.*'s study demonstrates the use of a predictive wave attenuation model to understand the level of protection provided by mangroves under different wave conditions, with different angles of approach, and with different spatial arrangements of the mangroves. Their study also demonstrates the potential for using such models in planning mangrove restoration and management: by varying the mangrove configurations and vegetation factor used, it is possible to quantify how the level of protection provided depends on the width of mangroves and the structure of the vegetation.
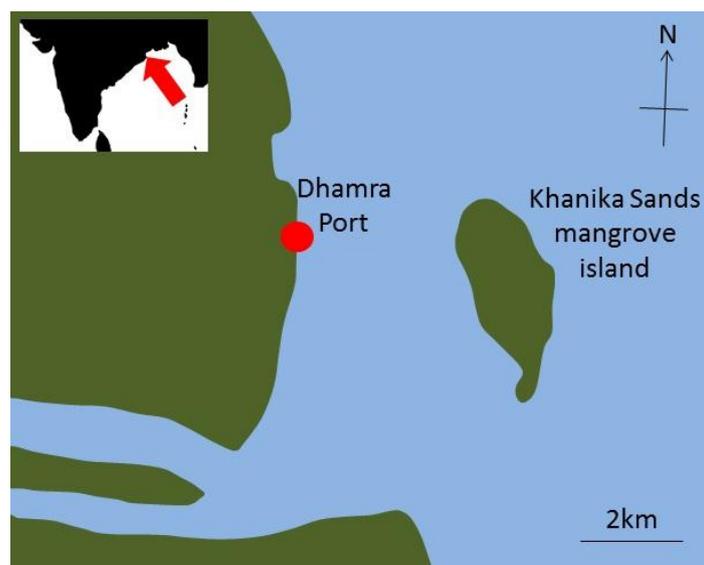
Figure 10. Dhamra Port and Khanika Sands mangrove island on the coast of Orissa, India. Adapted from Narayan (2009).
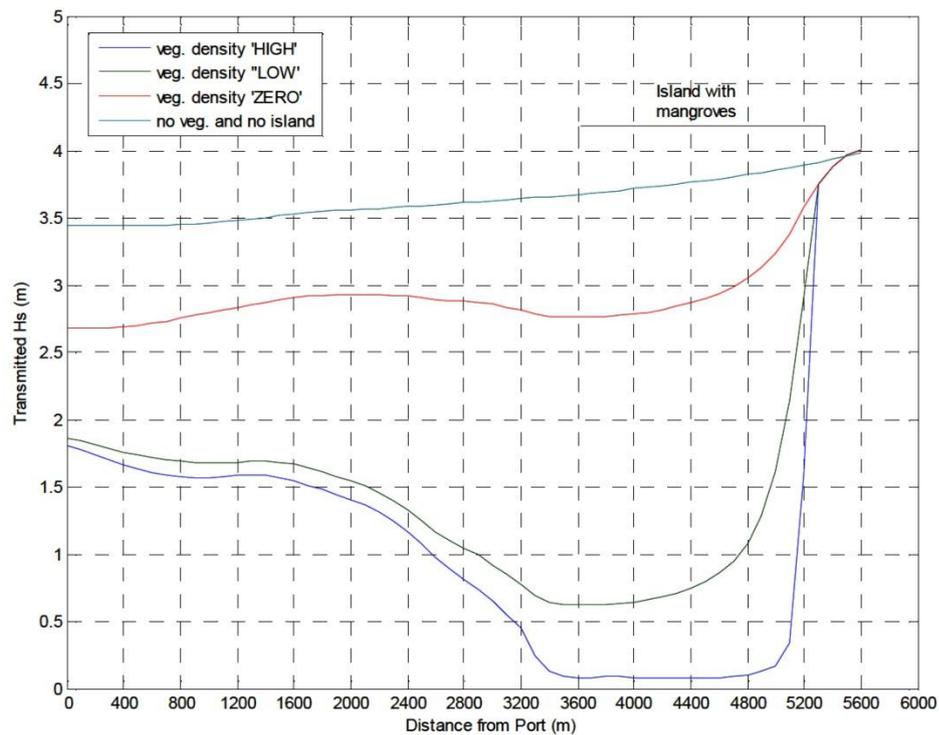
Figure 11. The transmitted wave heights (H_s = significant wave height) at different distances from the port for two different vegetation densities, compared with cases where there is no vegetation or no island, for waves with a return period of 25 years. Reproduced with permission, from Narayan (2009).

4.5.2 Case study 2: Determining the required width of a mangrove belt

Bao (2011) studied the reduction in wave height in mangrove forests in Vietnam, and created a statistical model relating wave attenuation to initial wave height, cross-shore distance and mangrove forest structure (as described in section 4.4). Bao used the model to calculate the minimum mangrove band width that would provide adequate protection from waves, and how this would vary for mangroves with different forest structures.

Based on Equation 5 in section 4.4, Bao (2011) derived the following equation to find the required width of a mangrove belt to attenuate waves by a certain amount (this is Equation 5 in Bao (2011) with the values of *a* and *b* substituted in from Equations 2 and 3 of Bao (2011)):

$$B_w = \frac{\ln(H_{safe}) - \ln(0.9899 H_0 + 0.3526)}{0.048 - (0.0016 \times \text{TH}) - (0.00178 \times \ln(TD)) - (\ln(CC))} \qquad \textbf{Eqn 6}$$

where B_W is the required mangrove band width (in metres) to achieve H_{safe}, the safe wave height (cm) for waves behind the mangroves, and *TH* is average tree height (m), *TD* is tree density (no. of trees / hectare), and *CC* is canopy closure (%).

Bao collated data on maximum wave heights in different regions along the coastline of Vietnam between January 2004 and December 2005 (collected by the Department of Hydrometeorology). Maximum wave heights ranged from 1.25 to 5.0m, so Bao chose 3.0m as a maximum wave height

to enter into the model (however it should be noted that the maximum measured wave height used to create Equation 5 was 70 cm, so further measurements are needed to ensure this equation is valid for larger waves). For the safe wave height, he used 30cm, based on the average observed wave height seen by 50 people working in aquaculture and agriculture in the study areas. Substituting these values into the model (Equation 6 above), the required band width becomes a function of forest structure:

$$B_w = \frac{-2.405}{0.048 - (0.0016 \times \text{TH}) - (0.00178 \times \ln(TD)) - (\ln(CC))} \quad \textbf{Eqn 7}$$

Bao then created a 'forest structure index' (FSI) based on the denominator of the right hand side of Equations 6 and 7:

Forest Structure Index (FSI) = - 0.048 + 0.0016 TH + 0.00178 ln (TD) + 0.0077 ln (CC)   **Eqn 8**

The required band width then becomes:

$$B_w = \frac{2.405}{FSI} \quad \textbf{Eqn 9}$$

Bao (2011) divided the forest structure index into 5 levels of wave prevention (Fig. 12 and Table 3). Table 3 allows the stakeholder to measure average tree height, tree density and canopy closure in a mangrove forest in Vietnam, apply Equation 8 to convert these measurements into the forest structure index, and then use the index to work out the required forest band width to provide protection from 3 m waves. This can help communities plan how wide a band of mangroves needs to be restored to protect the area behind from waves. However, it should be noted that further work is needed to assess the ability of mangroves to attenuate larger waves superimposed on top of a storm surge water level.

The benefits of this approach are its simplicity and ease of use. However, the wave climate is likely to vary significantly in different regions, and mangroves provide other services than just protection from waves. The necessary band width must also take into account the need to protect from other hazards (e.g. storm surges and tsunamis) and to provide other services, such as nursery areas for local fisheries.
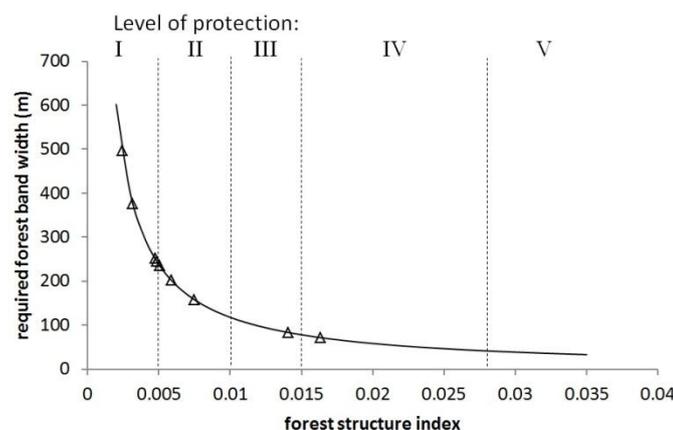
Figure 12. Theoretical curve created by Bao (2011) showing the relationship between the required forest band width and the forest structure index. Bao divided the index into 5 levels of protection (Table 3). The forest structure index of the sites used in Bao's study are shown (△). Adapted from Bao (2011).

Table 3. Bao's (2011) classification of mangrove forests by the amount of protection they can provide against wind waves. The sites in Bao's study mostly fell within levels I and II, with just 2 sites in levels III and IV (Figure 12).

Level of protection	Forest structure index	Level of protection	Required band width (m)
I	< 0.005	Very weak protection	> 240
II	0.005 – 0.010	Weak protection	120 – 240
III	0.010 - 0.015	Moderate protection	80 – 120
IV	0.015 – 0.028	Strong protection	40 – 80
V	> 0.028	Very strong protection	< 40

5. Conclusions

All studies have found that mangroves are able to attenuate wind and swell waves. The level of wave attenuation varies between 0.0014 /m and 0.011 /m (Table 2). These attenuation rates suggest that over 500 m of mangrove forest, wave height would be reduced by 50 to 99%. However, most studies have measured the attenuation of only relatively small waves (wave height < 70 cm), and further research is needed to measure the attenuation of larger wind and swell waves by mangroves.

Wave height reduction within a mangrove forest depends on the width of the forest, mangrove tree morphology relative to water depth, topography and wave height. Mangrove species with aerial roots are more effective at attenuating waves in shallow water, when the waves encounter the roots; species without aerial roots are more able to attenuate waves when the water level reaches the branches.

By quantifying the relationship between mangrove forest characteristics and the level of protection provided under different wave conditions, mangrove forests can be restored and managed in ways that optimise their coastal defence functions. In areas with small waves and dense mangrove forests, a thin band of mangroves may provide an adequate defence, while in a more exposed area with frequent storms and a more open mangrove forest structure, a much wider band will be required.

Two numerical models (WAPROMAN, Vo-Luong and Massel, 2008; SWAN, Suzuki *et al.*, 2011) have been used to model wave attenuation by mangroves, and the predictions of both models match observed wave attenuation reasonably well. However, they have only been tested against data from one location in Vietnam. Further tests are needed to increase confidence in their ability to predict wave attenuation in other locations, under different combinations of the controlling factors identified above (e.g. with different mangrove species or topography). One difficulty relates to measuring the drag coefficients needed by the models; more research is needed to measure these drag coefficients for common mangrove species experiencing waves under storm conditions.

The SWAN model has been used to simulate waves passing through a mangrove island in front of a port in Orissa, India (Narayan *et al.*, 2010). Such simulations can increase our understanding of the coastal defence functions currently provided by mangroves. By changing the forest widths and

configuration in the model, engineers can plan how to manage and restore mangroves as part of an integrated coastal defence strategy.

A regression model linking wave attenuation to easily measured forest characteristics (average tree height, tree density and canopy closure) has also been used to estimate how wide a band of mangroves should be restored in order to reduce wave heights from 3m to 0.3m on Vietnamese coasts (Bao, 2011). While this approach shows promise for use by non-experts at the local level, it currently relies on extrapolating wave attenuation data beyond measured wave heights, and has only been tested in Vietnamese mangroves.

While more research is needed, existing knowledge is sufficient to substantiate the claim that mangroves attenuate wind and swell waves. Appropriate management of mangrove areas could increase wave attenuation. This might include the protection of mangrove areas in key settings, or lead to the restoration or planting of mangroves in degraded and deforested settings, where local conditions have been shown to support the establishment of mangrove seedlings. To achieve the highest level of protection from wind and swell waves, a dense mangrove forest, including species with aerial roots, is recommended. The width of mangrove belt required will depend on the height of waves against which protection is needed and the density of mangrove vegetation through which the waves will pass.

6. Acknowledgements

7. References

Anderson, M.E., Smith, J.M. and McKay, S.K. (2011) Wave dissipation by vegetation. Coastal and Hydraulics Engineering Technical Note ERDC/CHL CHTN-I-82. Vicksburg, MS: US Army Engineer Research and Development Center. http://chl.erdc.usace.army.mil.chetn.

Asano, T., Debuchi, H. and Kobayashi, N. (1992) Interaction between water waves and vegetation. Proceedings of the 23rd International Conference on Coastal Engineering (chapter 207). ASCE. 2710-2723.

Asano, T., Tsutsui, S. and Sakai, T. (1989) Wave damping characteristics due to seaweed. Proceedings of the 35th Coastal Engineering Conference in Japan. JSCE. 138-142 (in Japanese).

Bao, T.Q. (2011) Effect of mangrove forest structures on wave attenuation in coastal Vietnam. Oceanologia 53, 807-818.

Booij, N., Holthuijsen, L.H. and Ris, R.C. (1996) The SWAN wave model for shallow water. Proceedings of the 25th International Conference on Coastal Engineering, Orlando, USA. 1, 668-676.

Booij, N., Ris, R.C. and Holthuijsen, L.H. (1999) A third-generation wave model for coastal regions. Part I: Model description and validation. Journal of Geophysical Research 104, 7649-7666.

Brinkman, R.M., Massel, S.R., Ridd, P.V. and Furukawa, K. (1997) Surface wave attenuation in mangrove forests. Proceedings of the Combined Australasian Coastal Engineering and Ports Conference, Christchurch, 1997, 941-946.

Burger, B. (2005) Wave attenuation in mangrove forests: numerical modelling of wave attenuation by implementation of a physical description of vegetation in SWAN. Masters thesis submitted to the Dep't of Civil Engineering and Geosciences, Delft University of Technology. URL: http://repository.tudelft.nl/view/ir/uuid%3A0e4c6450-fe5d-4693-9ca9-58da343448b7/.

Costanza, R., Perez-Maqueo, O., Luisa Martinez, M., Sutton, P., Anderson, S.J. and Mulder, K. (2008) The value of coastal wetlands for hurricane protection. Ambio 37(4), 241-248.

Dalrymple, R.A., Kirby, J.T. and Hwang, P.A. (1984) Wave diffraction due to areas of energy-dissipation. Journal of Waterway Port Coastal and Ocean Engineering - ASCE 110(1), 67-79.

Dean, R.G. and Dalrymple, R.A. (2002) Coastal Processes with Engineering Applications. Cambridge University Press, Cambridge, UK.

Fischenich, C. (2000) Resistance due to vegetation. EMRRP Technical Notes Collection (ERDC TN-EMRRP-SR-07), U.S. Army Engineer Research and Development Center, Vicksburg, MS. URL: http://www.wes.army.mil/el/emrrp.

Granek, E.F. and Ruttenberg, B.I. (2007) Protective capacity of mangroves during tropical storms: a case study from 'Wilma' and 'Gamma' in Belize. Marine Ecology-Progress Series 343, 101-105.

Hadi, S., Latief, H. and Muliddin (2003) Analysis of surface wave attenuation in mangrove forests. Proceedings of the ITB on Engineering Science 35B, 89-108.

Kinsman, B. (1965) Wind waves: their generation and propagation on the ocean surface. Prentice Hall, Englewood Cliffs, New Jersey.

Kobayashi, N., Raichle, A.W. and Asano, T. (1993) Wave attenuation by vegetation. Journal of Waterway Port Coastal and Ocean Engineering - ASCE 119(1), 30-48.

Krauss, K.W., Doyle, T.W., Doyle, T.J., Swarzenski, C.M., From, A.S., Day, R.H. and Conner, W.H. (2009) Water level observations in mangrove swamps during two hurricanes in Florida. Wetlands 29(1), 142-149.

Massel, S.R. (1996) Ocean surface waves: their physics and prediction. Advanced Series on Ocean Engineering (Volume 11). World Scientific Publishing Company, Singapore.

Massel, S.R., Furukawa, K. and Brinkman, R.M. (1999) Surface wave propagation in mangrove forests. Fluid Dynamics Research 24(4), 219-249.

Masselink, G., Hughes, M.G. and Knight, J. (2011) Coastal processes and geomorphology. Hodder Education, London, UK.

Mazda, Y., Magi, M., Ikeda, Y., Kurokawa, T. and Asano, T. (2006) Wave reduction in a mangrove forest dominated by *Sonneratia* sp. Wetlands Ecology and Management 14(4), 365-378.

Mazda, Y., Magi, M., Motohiko, K. and Hong, P.N. (1997a) Mangroves as a coastal protection from waves in the Tong King delta, Vietnam. Mangroves and Salt Marshes 1, 127-135.

Mazda, Y., Wolanski, E., King, B., Sase, A., Ohtsuka, D. and Magi, M. (1997b) Drag force due to vegetation in mangrove swamps. Mangroves and Salt Marshes 1, 193-199.

Mendez, F.J. and Losada, I.J. (2004) An empirical model to estimate the propagation of random breaking and nonbreaking waves over vegetation fields. Coastal Engineering 51(2), 103-118.

Möller, I. and Spencer, T. (2002) Wave dissipation over macro-tidal saltmarshes: Effects of marsh edge typology and vegetation change. Journal of Coastal Research SI36, 506-521.

Narayan, S. (2009) The effectiveness of mangroves in attenuating cyclone-induced waves. Masters thesis submitted to the Dep't of Civil Engineering and Geosciences, Delft University of

Technology. URL: http://repository.tudelft.nl/view/ir/uuid%3A6ece41e5-3609-45b5-902e-11b4aeca68c9/.

Narayan, S., Suzuki, T., Stive, M.J.F., Verhagen, H.J., Ursem, W.N.J. and Ranasinghe, R. (2010) On the effectiveness of mangroves in attenuating cyclone-induced waves. Proceedings of the International Conference on Coastal Engineering 32 (no page numbers). URL: http://journals.tdl.org/ICCE/article/view/1250.

Park, D. (1999) Waves, tides and shallow-water processes. Elsevier, Amsterdam, The Netherlands.

Pugh, D.T. (1987) Tides, Surges and Mean Sea-Level: A Handbook for Engineers and Scientists. John Wiley & Sons, Chichester, UK.

Quartel, S., Kroon, A., Augustinus, P., Van Santen, P. and Tri, N.H. (2007) Wave attenuation in coastal mangroves in the Red River Delta, Vietnam. Journal of Asian Earth Sciences 29(4), 576-584.

Suzuki, T., Zijlema, M., Burger, B., Meijer, M.C. and Narayan, S. (2012) Wave dissipation by vegetation with layer schematization in SWAN. Coastal Engineering 59(1), 64-71.

SWAN (2011) Simulating WAves Nearshore. Sourceforge. http://swanmodel.sourceforge.net/references/references.htm. Downloaded 17 November 2011.

TU Delft (2011) The official SWAN Home Page: http://www.swan.tudelft.nl. Downloaded 17 November 2011.

Thampanya, U., Vermaat, J.E., Sinsakul, S. and Panapitukkul, N. (2006) Coastal erosion and mangrove progradation of Southern Thailand. Estuarine, Coastal and Shelf Science 68(1-2), 75-85.

Vo-Luong, P. and Massel, S.R. (2006) Experiments on wave motion and suspended sediment concentration at Nang Hai, Can Gio mangrove forest, Southern Vietnam. Oceanologia 48(1), 23-40.

Vo-Luong, P. and Massel, S. (2008) Energy dissipation in non-uniform mangrove forests of arbitrary depth. Journal of Marine Systems 74(1-2), 603-622.

Woodroffe, C.D. (2002) Coasts: form, process and evolution. Cambridge University Press, Cambridge, UK.

Zhang, K.Q., Liu, H., Li, Y., Hongzhou, X., Jian, S., Rhome, J. and Smith III, T.J. (2012) The role of mangroves in attenuating storm surges. Estuarine, Coastal and Shelf Science 102-103, 11-23.